FEBS Letters 584 (2010) 3170–3178

journal homepage: www.FEBSLetters.org

Aloe emodin glycosides stimulates glucose transport and glycogen storage through PI3K dependent mechanism in L6 myotubes and inhibits adipocyte differentiation in 3T3L1 adipocytes

S. Anand, V.S. Muthusamy, S. Sujatha, K.N. Sangeetha, R. Bharathi Raja, S. Sudhagar, N. Poornima Devi, B.S. Lakshmi *

Centre for Biotechnology, Anna University, Chennai 600025, Tamilnadu, India

ARTICLE INFO

Article history:
Received 20 January 2010
Revised 14 May 2010
Accepted 4 June 2010
Available online 10 June 2010

Edited by Laszlo Nagy

Keywords:
Aloe emodin glycosides
Insulin resistance
Insulin signaling
Glucose transporter 4
Phosphatidyl inositol 3′ kinase
Glycogen synthesis

ABSTRACT

The present study discusses the efficacy of Aloe emodin-8-O-glycoside (AEG), a plant derived anthroquinone, on alleviating insulin resistance and augmenting glycogen synthesis in L6 myotubes and 3T3L1 adipocytes. Dose-dependent increase in glucose uptake activity (GUA) was observed in both cell lines. Immunoblot analysis revealed an insulin-like glucose transporting mechanism of AEG by activating key markers involved in the insulin signaling cascade such as insulin receptor beta IRβ, insulin receptor substrate1, 85 phosphatidyl inositol 3′ kinase (PI3K) and PKB. Glucose transporter 4 translocation was confirmed by determining the uptake of glucose in the presence of insulin receptor tyrosine kinase and PI3K inhibitors. AEG was found to enhance glycogen synthesis through the inhibition of glycogen synthase kinase 3β. In conclusion, AEG enhances glucose transport by modulating the proximal and distal markers involved in glucose uptake and its transformation into glycogen.
© 2010 Federation of European Biochemical Societies. Published by Elsevier B.V. All rights reserved.

1. Introduction

Insulin resistance is a key pathophysiological feature of type 2 diabetes. Impaired insulin secretion and free radical formation are the initial events triggering the development of insulin resistance and its causal relations with dysregulation of glucose and fatty acids metabolism. Although numerous oral hypoglycemic drugs exist alongside insulin, there is no promising therapy for NIDDM [1]. Some of the drugs such as sulphonylureas, and a few biguanides are valuable drugs for the treatment of hyperglycemia in NIDDM. However, these therapies are limited by their poor pharmacokinetic properties, secondary failure rates and accompanying side effects [2]. Hence in type 2 diabetic patients, the decreased ability of insulin to stimulate glucose disposal into muscle or adipose tissues results in insulin resistance [3]. Although the molecular basis of type 2 diabetes is poorly understood, it is well established that insulin signaling, including the activation of insulin receptor activity, is impaired in most of the patients with NIDDM.

In the present study, a pure compound was isolated from *Cassia fistula* which exhibited enhanced glucose uptake. The uptake of glucose and its mechanism of action were deciphered using an *in vitro* model. Based upon the glucose uptake activity the active extract was prioritized for purification. Bioassay aided column purification resulted in the isolation of a bioactive molecule which upon further structural characterization was elucidated as Aloe emodin glycosides (AEG) (Fig 1). Aloe emodin has been originally isolated from *Aloe vera* leaf [4] and from the root and rhizome of *Rheum palmatum* L. [5,6] and has also been reported for its antiproliferative effect on various cancer cells like merkel carcinoma cells [7,8] liver cancer cell lines (Hep G2 and Hep 3B) and human promyelocytic leukaemic cells (HL-60) [9]. It has been reported

Abbreviations: AEG, Aloe emodin glycosides; DMEM, Dulbecco's Modified Eagle Medium; DMSO, dimethyl sulphoxide; FBS, foetal bovine serum; KRPH, Krebs Ringer phosphate; SDS, sodium dodecyl sulphate; IRTK, insulin receptor tyrosine kinase; IRβ, insulin receptor beta; PTP1B, protein tyrosine phosphatase 1B; pNPP, p-nitrophenyl phosphate; IRS1, insulin receptor substrate1; PI3K, phosphatidyl inositol 3′ kinase; GLUT4, glucose transporter 4; GSK3β, glycogen synthase kinase 3β; PPARγ, peroxisome proliferator activator receptor gamma; C/EBP, CCAAT/enhancer binding protein; SREBP-1c, sterol regulatory element binding protein; ALP, alkaline phosphatase; NBT, nitroblue tetrazolium; BCIP, 5-bromo-4-chloro-3-indolylphosphate; WT, Wortmannin; GS, Genistein; CPM, counts per minute; RSG, rosiglitazone; LM, light microsome; PM, plasma membrane; SOV, sodium ortho vanadate; IDV, Integrative density value; Sc, Solvent control

* Corresponding author. Fax: +91 44 22350299.
E-mail addresses: lakshmibs@annauniv.edu, lakshmibs1@yahoo.com (B.S. Lakshmi).

0014-5793/$36.00 © 2010 Federation of European Biochemical Societies. Published by Elsevier B.V. All rights reserved.
doi:10.1016/j.febslet.2010.06.004

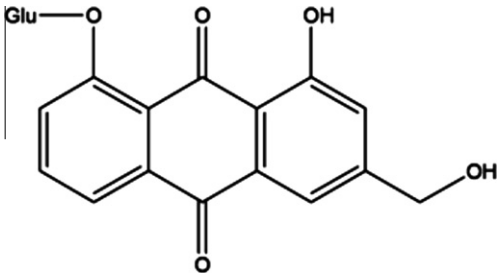

Fig. 1. Structure of the bio active pure compound chemically characterized as 8-(4, 5-dihydroxy-6 hydroxyl methyl-tetrahydro-pyran-3yloxy)-1-hydroxy-3-hydroxy-methyl-anthraquinone, with molecular formula $C_{21}H_{22}O_{10}$, molecular mass 434 and identified as Aloe emodin glycosides.

for anti-neuroectodermal tumor activity [10] and also as a potent hypotensive agent that leads to 79% fall in arterial blood pressure at a dose of 3 mg/kg [11]. The molecular mechanism of AEG was unknown and this is the first report for AEG from *Cassia fistula* that stimulates glucose uptake and glycogen storage via insulin signal transduction pathway.

2. Materials and methods

2.1. Chemicals and reagents

The chemicals were obtained from Sigma–Aldrich, St. Louis. All cell culture solutions and supplements were purchased from Life Technologies Inc. (Gaithersburg, MD, USA). Dulbecco's Modified Eagle Medium (DMEM) was obtained from GIBCO, BRL (Carlsbad, CA, USA). 2-DeoxyD-[1-^{3}H] glucose and hybond C membrane were obtained from Amersham Pharmacia Biotech, (Buckinghamshire, UK). Insulin, Genistein and Protein A Sepharose beads were obtained from Sigma–Aldrich (Andover, U.K.). Wortmannin was obtained from Calbiochem (Darmstadt, Germany). Rosiglitazone (RSG) was a kind gift from Dr. Reddy's Laboratories, Hyderabad. All the antibodies were procured from BD Pharmingen (San Diego, CA, USA) and Calbiochem. CytoTox 96 cytotoxicity assay kit was procured from Promega, USA.

2.2. Cell culture of L6 myotubes and 3T3L1 adipocytes

L6, a monolayer myoblast culture (obtained from ATCC-CRL-1458) and 3T3L1 preadipocytes (obtained from ATCC-CL-173) were cultured in DMEM with 10% foetal bovine serum (FBS) and supplemented with penicillin (120 units/ml), streptomycin (75 μg/ml), gentamycin (160 μg/ml) and amphotericin B (3 μg/ml) in a 5% CO_2 environment. For differentiation, the L6 cells were transferred to DMEM with 2% FBS for 4 days, post-confluence. The extent of differentiation was established by observing the multinucleate of cells. 3T3L1 preadipocytes grown in 24 well plates until 2 days post-confluence and the cells were induced by the differentiation medium (combination of 0.5 mM/l of IBMX, 0.25 μM/l of DEX and 1 mg/l of insulin in DMEM medium with 10% FBS) to differentiate into adipocytes. Three days after induction, the differentiation medium was replaced with medium containing 1 mg/ml insulin alone. The medium was subsequently replaced again with fresh culture medium (DMEM with 10% FBS) after 2 days the extent of differentiation was measured by monitoring the formation of multinucleation in cells.

2.3. Measurement of 2-deoxy-D-[1-^{3}H] glucose

L6 myoblasts and 3T3L1 preadipocytes grown in 24 well plate were subjected to glucose uptake as reported [12]. In brief, differentiated cells were serum starved for 5 h and were incubated with AEG for 24 h and then cells were either stimulated with 10 nM insulin or left untreated for 20 min. After experimental incubation, cells were rinsed once with HEPES buffered Krebs Ringer phosphate solution (118 mM NaCl, 5 mM KCl, 1.3 mM $CaCl_2$, 1.2 mM $MgSO_4$, 1.2 mM KH_2PO_4 and 30 mM HEPES and pH 7.4) and were subsequently incubated for 15 min in HEPES buffered solution containing 0.5 μCi/ml 2-deoxy-D-[1-^{3}H] glucose. The uptake was terminated by aspiration of media. Cells were washed thrice with ice cold HEPES buffer solution and lysed in 0.1% sodium dodecyl sulphate (SDS). The lysates were transferred to the plate with glass fiber paper and allowed to air dry. This plate was used to measure the cell-associated radioactivity by liquid scintillation counter. All the assays were performed in duplicates and repeated thrice for concordance. Results have been expressed as % glucose uptake with respective control. The % of glucose uptake was measured by applying counts per minute (CPM) values to the formula (Cells + AEG treated with insulin − Control (only cells) treated with insulin/Control (only cells) treated with insulin) × 100 and (Cells + AEG without insulin − Control (only cells) without insulin/Control (only cells) without insulin) × 100.

2.4. Bio activity guided structure elucidation

Based on the 2-deoxy-D-[1-^{3}H] glucose uptake studies the active methanolic extract was further purified and purity was established by HPLC. The structure of the active compound was determined by ^{1}H, ^{13}C nuclear magnetic resonance spectroscopy (NMR). The mass spectra confirmed the elemental composition of the compound. Amorphous yellow coloured powder (MeOH), IR (KBr): 3367, 2886, 1667, 1613, 1578, 1524, 1442, 1085. ^{1}H NMR (500 MHz, dimethyl sulphoxide (DMSO)d6) δ: 6.78 (1H, dd, H-2), 7.19 (1H, dd, H-4), 7.28 (1H, s, H-5), 7.46 (1H, m, H-6), 7.02 (1H, dd, H-7), 4.85 (2H, s, CH_{2-3}), 5.0 (1H, s, OH-1), 2.6 (1H, s, CH_2OH-3), 3.88 (1H, s, glu-CH), 3.96 (2H, s, glu-CH_2), 3.76 (1H, s, glu-CH), 3.04 (1H, s, glu-CH), 3.91 (1H, s, glu-CH), 3.62 (2H, s, glu-CH_2), 2.0 (4H, s, 4× glu-OH). ^{13}C NMR (100 MHz, DMSOd6) δ: 160.8 (C-1), 100.1 (C-2), 148.7 (C-3), 68.8 (C-CH2OH), 115.4 (C-4), 123.1 (C-2'), 145.2 (C-3'), 115.6 (C-5), 132.5 (C-6), 102.4 (C-7), 162.1 (C-8), 130.0 (C-6'), 110.2 (C-7'), 190.1 (C-9, carbonyl), 190.1 (C-10, carbonyl), 76.2 (glu-C-1), 67.5 (glu-C-2), 74.1 (glu-C-3), 69.2 (glu-C-4), 75.9 (glu-C-5), 65.2 (glu-C-6). Mass data *m/z*: 434 (M+). Based on the characterization, the isolated compound was found to be AEG (8-(4, 5-dihydroxy-6–hydroxyl methyl- tetrahydro-pyran-3yloxy)-1-hydroxy-3-hydroxymethyl-anthraquinone) and molecular formula was found to be $C_{21}H_{22}O_{10}$ with a molecular mass of 434.

2.5. Assessment of cytotoxicity by lactate dehydrogenase (LDH) release assay

Lactate dehydrogenase (LDH) release assay was performed [13] using a cytotox 96 assay kit (Promega) by quantitatively measuring LDH, a stable cytosolic enzyme released during cell lysis. The assay was done with 0.2×10^6 cells/0.2 ml/well, seeded in 96 well cell culture plates. Triton X-100 (0.05%) was used to induce maximal lysis. The plate was read at 492 nm in a scanning multiwell spectrophotometer. LDH was measured in supernatants by using the formula % LDH release = $[(OD_{sample} - OD_{control})/(OD_{TritonX} - OD_{control})] \times 100$.

2.6. 3T3L1 adipocyte differentiation inhibition and Adipo red staining

3T3L1 preadipocytes were induced by the combination of IBMX, DEX and insulin to differentiate into adipocytes as previous described (day 0). 72 h after induction, the differentiation medium was replaced with 10% FBS–DMEM containing 1 mg/l insulin for

48 h (day 5). The medium was replaced again with fresh culture medium for 48 h (day 7). The degree of the differentiation of the cells was investigated by adding AEG at logarithmic doses ranging from 1 pg/ml to 1 μg/ml from day 0, a period of time which covered the entire induction and post induction stages. Alternatively, preadipocytes were maintained with fresh FBS–DMEM every other day for the whole spectrum of induction period [14]. AdipoRed® lipid staining assay (Lonza Walkersville Inc.) was performed at the end of the induction period to monitor the degree of differentiation as described above. Photomicroscopic evaluation was also carried out for the comparison of triglyceride accumulation.

2.7. PTP1B inhibition assay

The enzymatic assay was carried out in sodium acetate buffer, in a 96 well format. The initial rate of protein tyrosine phosphatase 1B (PTP1B)-catalyzed hydrolysis of p-nitrophenyl phosphate (pNPP) was measured by following the absorbance change at 405 nm. Purified recombinant human PTP1B from Biomol was used for the study. Effect of AEG on PTP1B enzyme inhibition was determined at fixed enzyme and substrate concentration.

2.8. Inhibitor studies

Glucose uptake analysis in presence of inhibitors such as genistein, wortmannin was performed as explained [15,16]. Briefly, L6 myotubes were serum starved for 5 h and pre-treated with the inhibitors wortmannin (100 nM) and genistein (50 μM) respectively for 30 min. AEG was incubated for 24 h and their effect on glucose uptake was measured as mentioned earlier.

2.9. Immunoprecipitation and immunoblotting

L6 myotubes were treated with optimum concentrations of AEG after serum deprivation. Total cell lysates were prepared as reported previously [17]. Anti insulin receptor substrate1 (IRS1) antibody was added to the eppendorf tube containing the cold lysates and incubate at 4 °C for 1 h. Protein A Sepharose (50 μl) beads was activated by washing with cold lysis buffer (500 μl) and centrifuged at 10 000×*g* for 30 s twice. Finally, 50 μl of washed Protein A Sepharose slurry was added to total protein (125 μg) isolated from AEG treated L6 myotubes and immunoprecipitated for 1 h at 4 °C on a rocking platform. The eppendorf was spun at 10 000×*g* for 1 min at 4 °C for washing and this step was performed 3–5 times with 500 μl of lysis buffer. After the last wash, 50 μl of 1× laemmli sample buffer was added to bead pellet, vortexed and heated to 90–100 °C for 10 min. This was spun at 10 000×*g* for 5 min and the resultant supernatant was loaded onto 10% SDS–polyacrylamide gel, electrophoretically transferred onto a nitrocellulose membrane. Then, the membrane was blocked overnight in blocking agent (5% skimmed milk) at 4 °C and incubated with desired primary antibody for 2 h. After washing, membrane was incubated with alkaline phosphatase conjugated secondary antibody in 5% BSA in PBS for 1 h at room temperature. Then the blot was washed with PBS thrice, each 5 min and the blot was developed with the nitroblue tetrazolium/5-bromo-4-chloro-3-indolylphosphate NBT/BCIP chromogenic agent and photographed. The immunoblots were probed with the respective primary antibody with phosphorylated and non-phosphorylated form of insulin receptor beta (IRβ), IRS1, phosphatidyl inositol 3′ kinase (PI3K), PKB, glucose transporter 4 (GLUT4), glycogen synthase kinase 3β (GSK3β) and peroxisome proliferator activator receptor gamma (PPARγ), followed by specific secondary antibody and visualized using a chromogenic substrate. The density of the protein bands were quantitated by densitometry scanning (Chemi Imager 4400, Alpha Innotech Corporation).

2.10. Sub-cellular membrane fractionation

Sub-cellular fractionation of plasma membranes was carried out as described [18] with some modifications. Briefly, L6 myotubes after treatment with AEG was washed and re-suspended in buffer I (250 mM/l sucrose, 5 mM NaN_3, 20 mM HEPES, 200 μM/l PMSF, 1 μM/l pepstatin, 1 μM/l aprotinin and 2 mM/l EGTA, pH 7.4). Cell lysate was homogenized using 20 strokes of a Dounce homogenizer (0.5 cycles, 10 pulses; 2 min each and lag time of 1 min for each pulse). Lysates were centrifuged at 750×*g* for 5 min at 4 °C to remove cell debris. The plasma membrane (PM) fraction was obtained by centrifugation of the resulting supernatant at 30 000×*g* for 40 min at 4 °C. The resultant pellet was re-suspended in buffer I and this constitutes the PM fraction. Supernatant was removed and centrifuged at 100 000×*g* for 75 min at 4 °C to generate the cytosol fractions. The light microsome (LM) pellet was re-suspended in buffer I and assayed for soluble protein content by Bradford's assay. The membrane fractions were subjected to electrophoresis on 10% SDS–PAGE, transferred to nitrocellulose membranes, and immunoblotted with anti-GLUT4 antibody.

2.11. Glycogen synthesis

Glycogen level was measured as described early [19]. In brief, completely differentiated L6 myotubes were serum starved for 5 h and treated with different concentrations of AEG for 24 h. After the specified time point, cells were either stimulated with 10 nM insulin or left untreated for 20 min and then pulsed with 1 μCi/ml [^{14}C] glucose in genistein (GS) buffer (2.5 mM glucose, 0.1% BSA, 25 mM HEPES, pH 7.4) and incubated for 30 min at 37 °C. The cells were then lysed in 30% KOH and 20 mg/ml of carrier glycogen was added and heated for 30 min at 70 °C. Glycogen synthesized was then precipitated using ice cold ethanol at 20 °C for 24 h and centrifuged at 2000×*g* for 10 min. The glycogen pellet was dried and dissolved in 200 μl of water and counted in liquid scintillation counter. The % of glucose incorporation into glycogen was measured by applying CPM values to the formula (Cells + AEG treated with insulin − Control (only cells) treated with insulin/Control (only cells) treated with insulin) × 100 and (Cells + AEG without insulin − Control (only cells) without insulin/Control (only cells) without insulin) × 100.

2.12. Statistical analysis

Statistical analysis was performed using GraphPad Prism, 4.03 (San Diego). One way analysis of variance (ANOVA) followed by Dunnett's post hoc used for other parameters. Data were expressed in means ± S.E.M. The criterion for statistical significance was $P < 0.05$.

3. Results

3.1. AEG stimulates glucose uptake in L6 myotubes and 3T3L1 adipocytes at 24h

In an endeavor to identify a small molecule that could stimulate glucose uptake like insulin, a cell based assay using L6 myoblast and 3T3L1 preadipocytes was performed. These cells can be induced to differentiate into myotubes and adipocyte phenotype, as described previously thus serving as efficient models to measure glucose disposal [20]. The differentiated cells were treated with AEG isolated from *Cassia fistula* and incubated for 24 h. After the incubation period the cells were assessed for insulin stimulated 2-deoxy-D-[1-^{3}H] glucose uptake.

AEG (Fig. 1) isolated from *Cassia fistula* methanolic extract (CFME), enhanced glucose uptake in L6 myotubes and 3T3L1

adipocytes in a concentration dependent manner and the optimum dose exhibiting maximum activity was found to be 100 pg/ml which was used for further studies (Fig. 2A and B). Additionally, AEG was found to be non-toxic (less than 20% toxicity) even at high concentration (10 μg/ml) (Fig. 3).

3.2. Effect of AEG on the inhibition of adipocyte differentiation

Two-day post confluent, 3T3L1 preadipocytes were induced for differentiation in the presence of logarithmic doses of AEG ranging from 1 pg/ml to 1 μg/ml. Intracellular lipid content by AdipoRed® staining was performed to measure the degree of adipocyte differentiation. When AEG was added to the preadipocytes in the presence of differentiation medium only basal level lipid accumulation was observed (Fig. 4A). Cytotoxicity assay by LDH release measurement revealed that the AEG treated preadipocytes were 90% viable for the whole duration of the assay period. The differences in lipid accumulation of AEG treated adipocytes were photomicrographed at 10x magnification (Fig. 4B). However, AEG did not alter the PPARγ phosphorylation (Fig. 4C). The expression levels of these proteins were subsequently semi-quantified by densitometric analysis (Fig. 4D).

3.3. Effect of AEG on IRTK and PI3K inhibition

To investigate whether AEG stimulated glucose uptake is mediated through tyrosine kinase dependent pathway, glucose uptake assay was performed with genistein (a tyrosine kinase inhibitor) for 30 min, followed by treatment with insulin (100 nM) or AEG for 24 h (Fig. 5). Genistein inhibited both insulin and AEG stimulated glucose uptake. Hence the result suggested that AEG mimics insulin, by acting via the tyrosine kinase dependent pathway. The activation of PI3K is necessary for insulin stimulated glucose transport [21]. To investigate whether AEG stimulated glucose uptake is mediated through PI3K activation, we examined the effects of

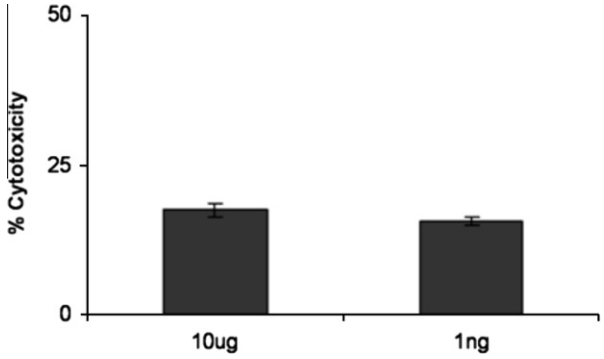

Fig. 3. Influence of AEG on the cytotoxicity in L6 myotubes. Cytotoxic effect of AEG measured on L6 myotubes as indicated doses of AEG at 24 h. Cytotoxicity was expressed as % LDH release. Data represent the means ± S.E.M. of triplicates of three independent experiments. $^{*}P < 0.05$ as compared with untreated control group.

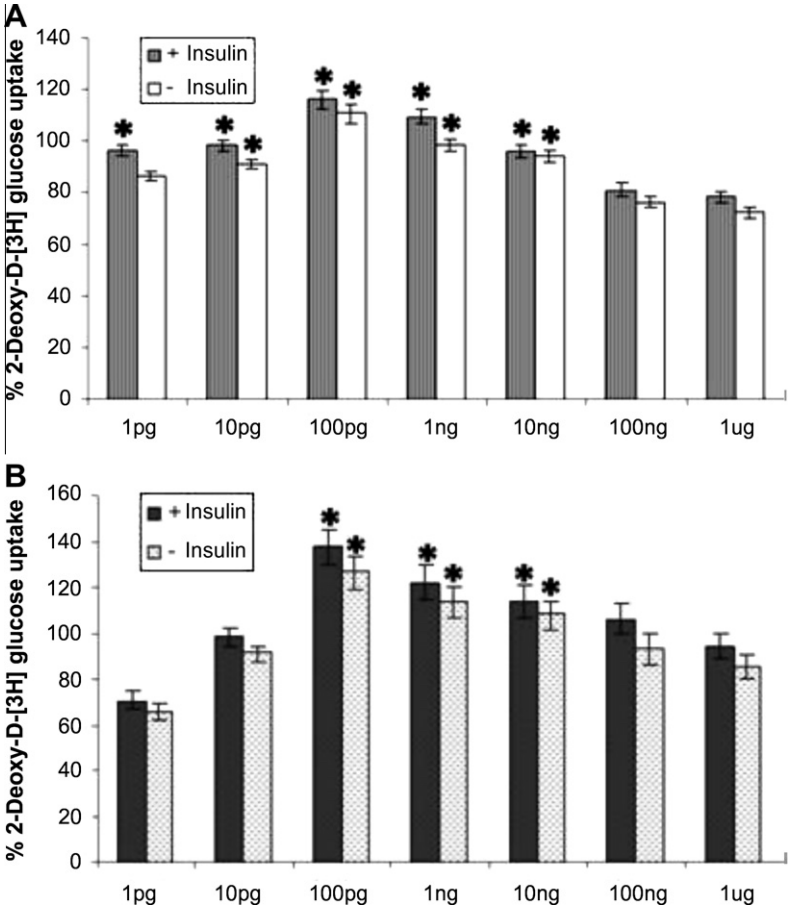

Fig. 2. Dose response analysis of AEG on 2-deoxy-D-^{3}[H] glucose uptake on L6 myotubes and 3T3L1 adipocytes. (A and B) The cells were treated with different concentrations of AEG for 24 h in the presence and absence of insulin as mentioned in Section 2. After experimental incubation, 2-deoxy-D-^{3}[H] glucose (0.5 μCi/ml) was added to the cells for 20 min and the uptake was measured. The results were expressed as % glucose uptake with their respective controls which are cells treated with insulin (10 nM) and DMSO (solvent control) and cells and DMSO (solvent control) without insulin. The optimum concentration of AEG was found to be 100 pg/ml for both L6 and 3T3L1. All the data were expressed as means ± S.E.M. of three independent experiments. $^{*}P < 0.0001$ as compared with respective control group.

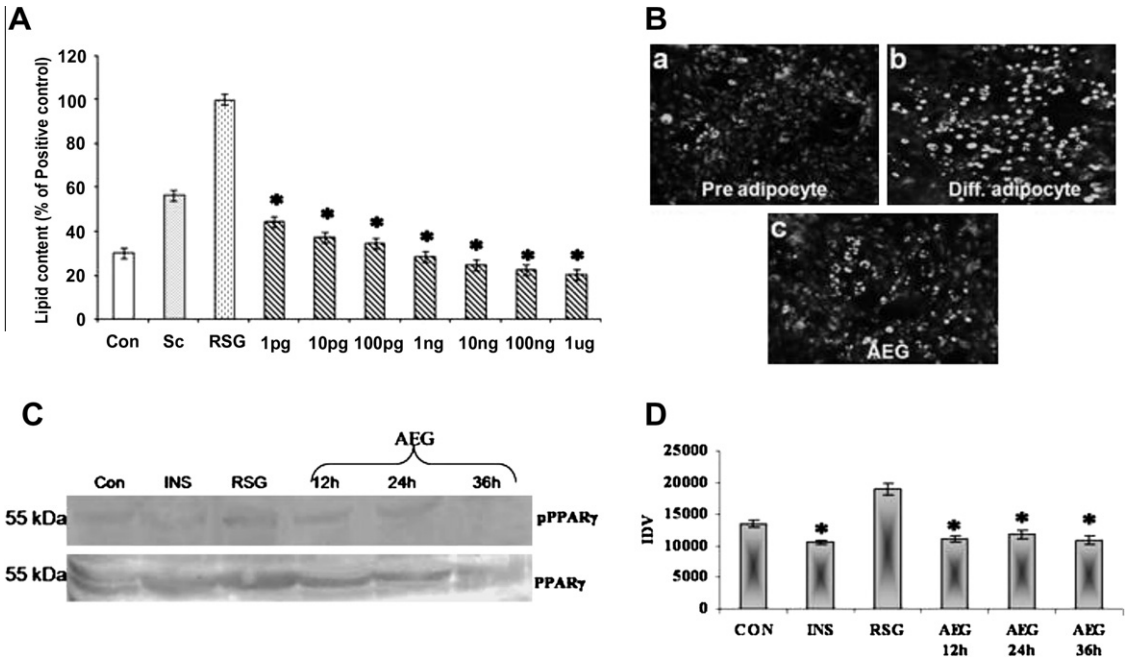

Fig. 4. (A–D) Effect of AEG on lipid accumulation in 3T3L1 adipocyte after differentiation induction. (A) Two-day postconfluent 3T3-L1 cells were differentiated according to the protocol followed by treatment with described doses of AEG or vehicle for 2 days. Eight days after induction of differentiation, cells were assayed for total triglyceride content using Adipored reagent. Preadipocytes were separately maintained as per the protocol indicated. Data shown reflect the means ± S.E.M. of triplicates of two determinations. $^{*}P < 0.0001$ as compared with preadipocytes group. Photomicrographs were documented to evaluate the morphological changes of adipocytes at magnification ×100. (B) (a) Pre adipocyte (b) differentiation induced (c) differentiation induced + AEG. (C) Western blot analysis of PPARγ using whole cell lysate of AEG treated with L6 myotubes at different time points from 12, 24 and 36 h. (D) The protein was subsequently quantified by densitometry analysis. $^{*}P < 0.05$ as compared with untreated control group.

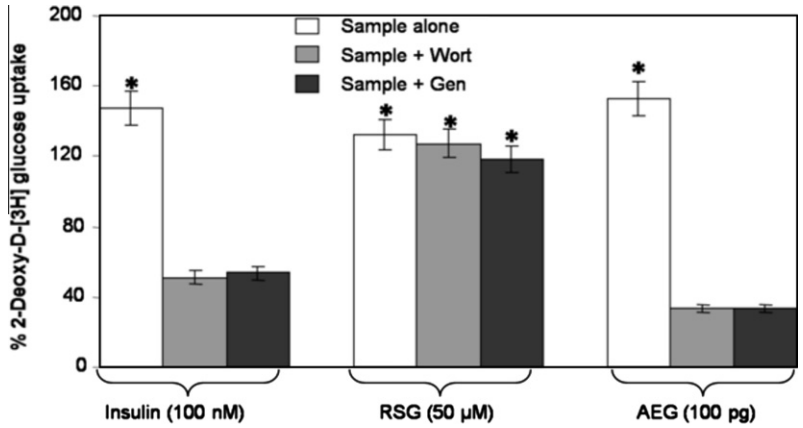

Fig. 5. Glucose transport behavior of AEG in the presence of inhibitors. L6 myotubes were pre-treated with AEG in addition of 100 nM Wortmannin (WT) – PI3K inhibitor and 50 μM Genistein (GS) IRTK inhibitor at the concentration indicated and subjected to glucose uptake assay. Inhibitors suppressed the glucose uptake of AEG, which showed uptake similar to that of positive control insulin. Rosiglitazone served as negative control and did not alter the glucose uptake in the presence of inhibitor. The results were expressed as % change in glucose uptake with respect to the control. Data represent the means ± S.E.M. of triplicates of two independent experiments. $^{*}P < 0.05$ as compared with untreated control group.

wortmannin, a selective inhibitor of PI3K, on AEG stimulated glucose uptake. Interestingly, AEG stimulated glucose uptake in L6 myotubes declined (74% inhibition) on treatment with 100 nM wortmannin (Fig. 5). These results suggest that the signal transduction leading to glucose uptake by AEG is primarily mediated via PI3K pathway.

3.4. Effect of AEG on PTP1B inhibition

PTP1B has been implicated as the negative regulator of the insulin signaling pathway. It dephosphorylates the specific phosphotyrosine residues on the insulin receptor thereby reducing the insulin receptor tyrosine kinase (IRTK) activity. Hence inhibition of this enzyme (PTP1B) would be validated as a therapeutic target in the treatment of NIDDM as well as obesity. AEG was examined for its effect on PTP1B inhibition at its optimum concentration. It was found that AEG exhibited only a moderate PTP1B inhibition level as compared to the positive control SOV (sodium ortho vanadate) (Fig. 6).

3.5. Effect of AEG on insulin signaling and GLUT4 translocation

Immunoprecipitation and immunoblot analysis revealed that AEG (100 pg/ml) treatment on L6 myotubes for 24 h significantly

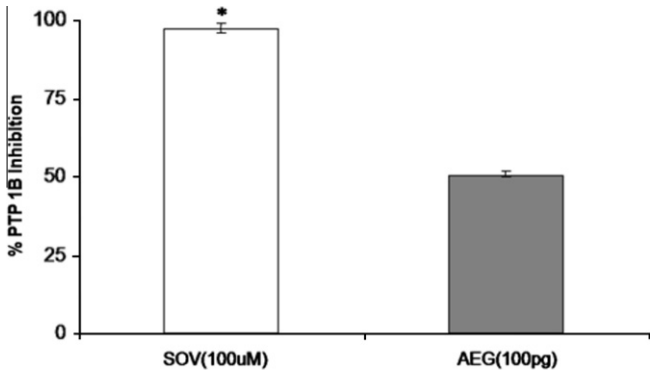

Fig. 6. Effect of AEG on inhibition of PTP1B enzyme. AEG exhibited moderate inhibition of PTP1B enzyme as compared with positive control sodium ortho vanadate which showed maximum inhibition of PTP1B enzyme. Data represent the means ± S.E.M. of triplicates of two independent experiments. $^{*}P < 0.0001$ as compared with untreated control.

enhanced the phosphorylated level of key insulin signaling markers such as IRβ, IRS1 and PI3K when compared to untreated cells (Fig. 7A). The expression levels of these proteins were quantified semi-quantitatively by densitometry analysis (Fig. 7B). The translocation pattern in response to AEG on L6 myotubes at 24 h was analyzed (Fig. 8B). The AEG was able to translocate GLUT4 from light microsomes to plasma membrane (PM). Insulin and RSG were used as the positive controls. The majority of the GLUT4 translocating to PM upon AEG treatment similar to the positive controls was observed (Fig. 8B and C). To determine the other downstream protein kinase in insulin signaling, the role of PKB phosphorylation was examined (Fig. 9A). A significant inhibition of GSK3β through enhanced phosphorylation was observed in L6 myotubes treated with AEG for 24 h. The results were quantified by densitometric analysis (Fig. 9B).

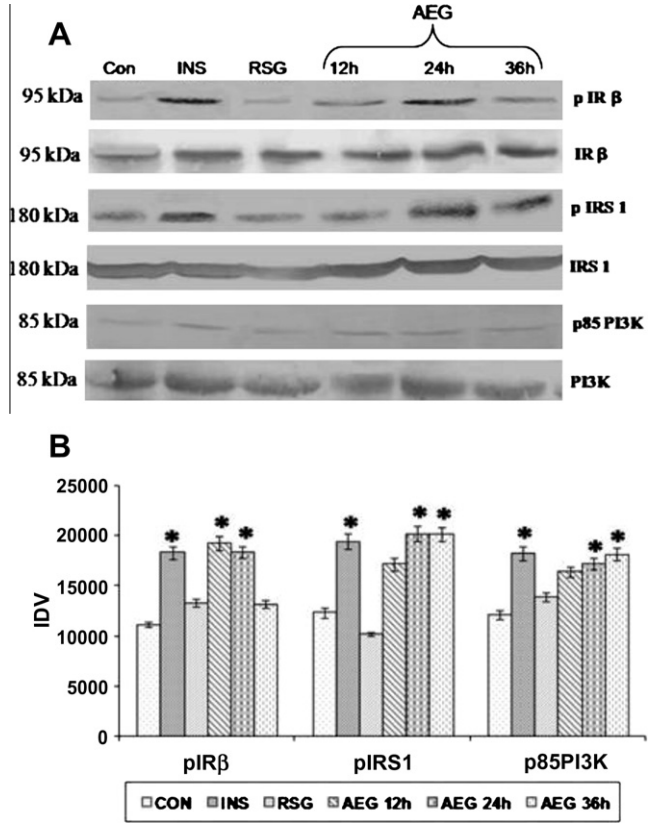

Fig. 7. (A) Western blot analysis of insulin signaling markers IRβ, IRS1, PI3K, using whole cell lysate of AEG treated with L6 myotubes at different time points from 12, 24 and 36 h. (B) The signaling intensities for semi-quantitative analysis of IRβ, IRS1, and PI3K protein expression were quantified by densitometry. Bars represent the means ± S.E.M., $n = 3$ and a representative blot is depicted here. $^{*}P < 0.05$ as compared with untreated control group.

3.6. Effect of AEG on glycogen synthesis activation

Insulin stimulated transformation of glucose into glycogen was significantly high upon AEG treatment (121% at 100 pg/ml) (Fig. 10). Similarly, AEG showed a considerable increase in glycogen synthesis even in the absence of insulin stimulation. Effect of AEG in glycogen synthesis was compared with positive control insulin (100 nM).

4. Discussion

The current study reveals the glucose transporting efficacy of Aloe emodin glycosides and demonstrates the molecular mechanism involved in mediating insulin signaling pathway through an *in vitro* model. Pathogenesis of NIDDM involves a combination of genetic and environmental factors, which cause insulin resistance in target tissues [22]. Skeletal muscle is the primary site for insulin stimulated glucose uptake and a large part of the glucose incorporated into muscle cells is deposited as glycogen in response to insulin. Thus, glucose uptake and glycogen synthesis in skeletal muscle play a pivotal role in blood glucose homeostasis. The importance of IRTK and PI3K has been well established in the insulin downstream signal transduction particularly by the activation of insulin receptor through autophosphorylation followed by sequential events of PI3K activation [23] ultimately resulting in GLUT4 translocation [24]. The impaired glucose uptake linked with defect in GLUT4 translocation and impaired insulin signaling cas-

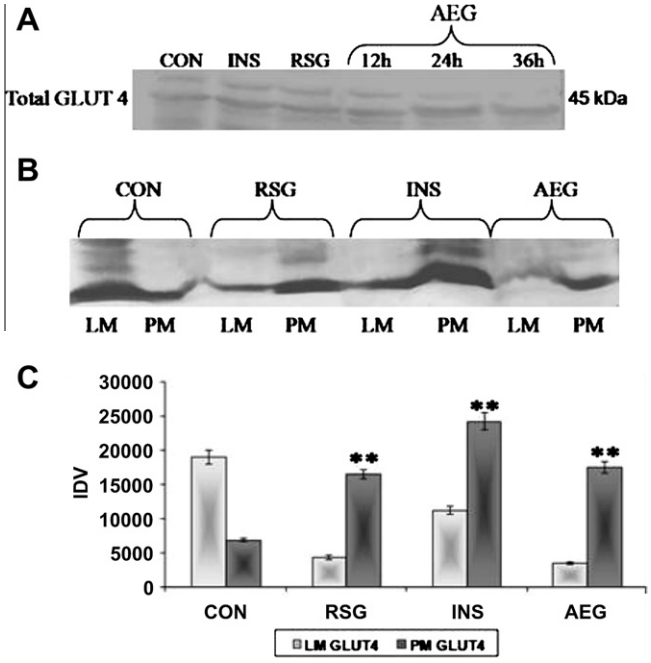

Fig. 8. (A) Western blot analysis of total GLUT4 of AEG at different time points from 12, 24 and 36 h on L6 myotubes. (B and C) Effect of AEG on translocation of GLUT4 at 24 h on L6 myotubes semi-quantitatively. Insulin (100 nM) and rosiglitazone (50 μM) were used as positive controls. Bars represent the means ± S.E.M., $n = 3$ and a representative blot is depicted here. $^{**}P < 0.05$ as compared with untreated control group.

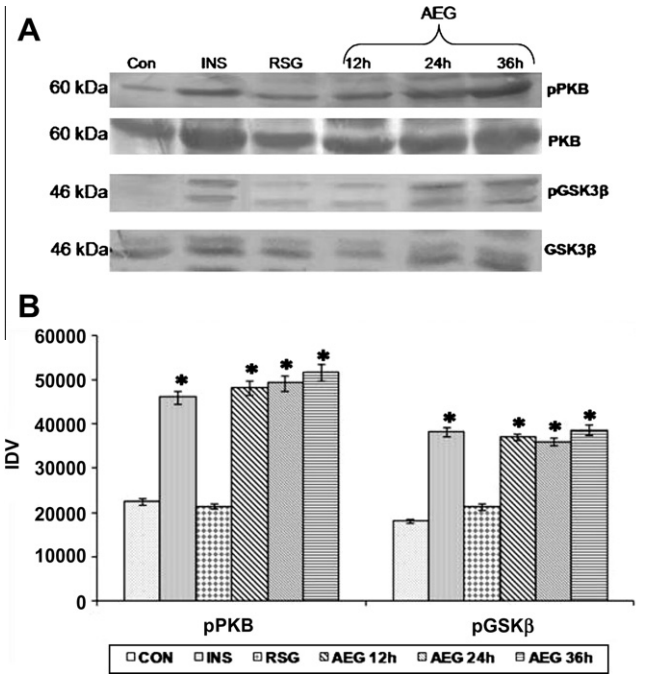

Fig. 9. Effect of AEG on (A) protein expression of PKB, GSK3β treated with L6 myotubes at 12, 24 and 36 h. (B) The protein expressions were normalized using representative non-phosphorylated proteins. Bars represent the means ± S.E.M. of PKB and GSK-3β. *$P < 0.05$ as compared with untreated control group.

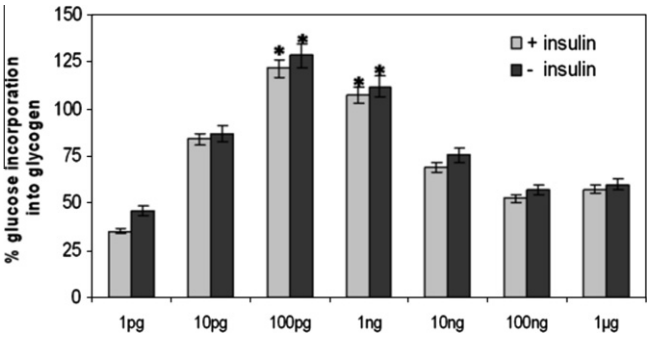

Fig. 10. Dose response analysis of glycogen synthesis in AEG treated cells at 24 h in the presence and absence of insulin. The results were expressed as% of glucose incorporated into glycogen with their respective controls which are cells treated with insulin (10 nM) and DMSO (solvent control) and cells and DMSO (solvent control) without insulin. Data represent the mean ± S.E.M. of triplicates of two independent experiments. *$P < 0.05$ as compared with respective control group.

cade has been proven in patients with type 2 diabetes [25]. The serine/threonine kinase Akt, also known as protein kinase B (PKB) could play a role in the activation of glucose uptake and glycogen synthesis in L6 myotubes [26], in addition to being a central intermediate for many of the insulin and growth factor responses downstream of PI3K. Akt has been identified as one of the insulin responsive kinases that phosphorylates glycogen synthase kinase-3 (GSK-3) [27]. Subsequent studies have demonstrated that Akt has a role in promoting GLUT4 translocation in adipocytes [28], glucose transport and glycogen synthesis in L6 myotubes [29].

An insulin mimetic molecule from a fungus activating IRTK and PI3K [30] has been isolated. Previous studies have postulated that triterpenoids act as insulin-mimicker by activating IRβ, IRS1 and GLUT4 translocation [31,32] which coincides well with the results obtained with AEG treated cells. 2-deoxy-D-^{3}[H] glucose uptake assay was performed by AEG in a dose dependent manner in both L6 myotubes and 3T3L1 adipocytes. AEG exhibited significant increase in glucose uptake by L6 myotubes and 3T3L1 adipocytes at 120% and 140% respectively. The percentage uptake was calculated on par with the positive control RSG which showed an uptake of 165%. Lactate dehydrogenase (LDH) release in L6 myotubes on treatment with AEG at 24 h incubation shows that AEG is non-toxic even at higher concentrations.

Insulin exerts its biological effect upon binding with insulin receptor (IR) thereby stimulating the downstream signaling events that lead to enhanced glucose uptake. In skeletal muscle, it potentiates the glucose transport through PI3K mediated and non-PI3K mediated pathways. Alterations in the level of IR or defects in its signal transduction pathway have been found in diabetic patients associated with decreased levels of IRβ, IRS-1 and PI3K [33]. To reveal the molecular mechanism of AEG, in augmenting glucose transport, and its effect on phosphorylated level of IRβ, IRS1 and PI3K western blot analysis was performed. Pessin et al. have emphasized the major role of PI3K in insulin signaling pathway and in regulating insulin-mediated glucose transport [34]. To examine whether AEG stimulates glucose transport in a PI3K dependent manner, western blot analysis and phospho-detect p85PI3K were employed. The expression of PI3K is substantiated by the enhanced expression of the catalytic subunit of PI3K on treatment with AEG. A time dependent analysis showed an increase in the phosphorylation of IRβ, IRS1, PI3K clearly indicating that AEG acts through a PI3K dependent pathway. RSG was used as the negative control since it upregulates glucose uptake in a PI3K independent manner. The above finding confirms that the increased uptake of glucose exhibited by AEG is through the activation of GLUT4. This observation also correlates with the inhibitor studies performed using genistein (IRTK inhibitor) and wortmannin (PI3K inhibitor). In conclusion, it is observed that the insulin like activity of AEG in upregulating glucose transportation is IRTK and PI3K mediated.

GLUT4 is the predominant glucose transporter among various isotypes of glucose transporters in insulin sensitive tissues like skeletal muscle and adipocytes, which transports glucose from blood into tissue. Decrease in the translocation of GLUT4 to the PM has been a major cause of insulin resistance. It is therefore essential to activate GLUT4 in skeletal muscle to alleviate insulin resistance and to maintain blood glucose homeostasis. Metformin and troglitazone enhance insulin stimulated glucose uptake by increasing the cell surface GLUT4 content [35]. Semi-quantitative analysis of GLUT4 translocation was performed by sub-cellular fractionation of cell lysates in order to separate the LM and the PM. For assessing whether the increased glucose uptake stimulated by AEG was due to the translocation of GLUT4, the amounts of GLUT4 present in LM and PM was measured after the treatment of AEG on L6 myotubes at 24 h. AEG was able to translocate majority of the GLUT4 from light microsomes to PM. Insulin and RSG served as the positive control and were able to translocate GLUT4 to PM at 15 min and 24 h respectively. The process of translocation of GLUT4 to PM was quantified using densitometry scanning.

Further, probing the role of insulin in glycogen synthesis, Akt/PKB is a downstream event of PI3K and plays an important role in insulin-mediated glucose transport as well as glycogen synthesis [36]. Activated PKB increases glycogen synthesis through an inhibition of GSK3β [37,38]. Constitutively active GSK3β is the major contributor of insulin resistance and it serves as a gatekeeper by negatively regulating the insulin receptor signal in the absence of stimulus. So identifying a potent molecule that activates glucose storage through an activation of PKB and inhibition of GSK3β would be an interesting finding. Based on this, AEG was examined for its role in PKB and GSK3β phosphorylation. AEG showed signif-

icant increased phosphorylation of PKB and GSK3β exhibiting its prominent role in modulating glycogen synthesis through an activation of PKB and inactivation of GSK3β.

In addition, the effect of AEG on adipogenesis was assessed in 3T3L1 adipocytes. Adipogenesis, the process of preadipocyte differentiation into adipocytes is controlled by various positive and negative regulators such as hormones, adipogenic genes, adipokines and growth factors [39]. PPARγ, CCAAT/enhancer binding protein and sterol regulatory element binding protein families are well-documented primary adipogenic transcription factors involved in adipocyte differentiation and among them PPARγ is the most extensively studied and clinically validated adipogenic gene for therapeutic utility in type 2 diabetes [40]. Upregulation of PPARγ gene by thiazolidinediones in skeletal muscle has been reported to improve insulin sensitivity and glucose uptake [12]. Although relatively beneficial for their anti-diabetic action, thiazolidinediones have been reported to cause abnormalities in lipid metabolism and cardiac side-effects [41]. In the present analysis, 3T3L1 adipocytes incubated with AEG clearly revealed a significant decrease in lipid droplets formations and did not alter the PPARγ protein expression. AEG also inhibits adipocyte differentiation in 3T3L1 adipocytes that correlates with our observation of PPARγ phosphorylation. Hence it can be concluded that AEG exhibits glucose-lowering efficacy without inducing adipogenesis.

Since the observed effect of AEG on insulin signaling markers, glucose uptake, adipogenesis and glycogen synthesis are distinctive activity profile for both PTP1B inhibitors [42] and AMPK activators [43], AEG was assessed for PTP1B inhibition and compared with known PTP1B inhibitor (SOV). The tyrosine phosphorylation of the insulin receptor and its substrates is countered by dephosphorylation of the protein phosphatases like protein phosphatase 1B (PTP1B). In case of insulin resistance, the dephosphorylation of these phosphatases exerts the phosphorylation of insulin receptor and its substrates [44,45]. A decrease in adipogenesis with a down regulation of all adipogenic genes in animals ablated with PTP1B was postulated to play a pivotal role in the development of obesity [46]. The moderate effect of AEG on PTP1B inhibition eliminates the possibility of AEG as a potent PTP1B inhibitor. In conclusion, AEG exhibits insulin mimetic activity by activating IRβ, IRS1, p85 subunit of PI3K, PKB and GLUT4 translocation and inhibiting GSK3β phosphorylation, thus upregulating glucose uptake and storage respectively in a PI3K dependent pathway. Based on these inferences AEG could be validated as an anti-diabetic molecule deficient of adipogenic activity providing an opportunity to develop a novel class of drug that is more effective in the treatment of insulin resistance.

References

[1] Sumana, G. and Suryawanshi, S.A. (2001) Effect of *Vinca rosea* extracts in treatment of alloxan diabetes in male albino rats. Indian J. Exp. Biol. 39, 748–758.

[2] Melander, A. (1988) Non-insulin dependent diabetes mellitus treatment with Sulphonylureas in: Clinical Endocrinology and Metabolism (Natrass, M. and Hale, P., Eds.), pp. 443–453, Balliere-Tindall, London.

[3] Kahn, C.R. (1994) Banting lecture. Insulin action, diabetogenes, and the cause of type 2 diabetes. Diabetes 43, 1066–1084.

[4] Hamman, J.H. (2008) Composition and applications of *Aloe vera* leaf gel. Molecules 13, 1599–1616.

[5] Tsai, T.H. and Chen, C.F. (1992) Ultra violet spectrum identification of emodin in rabbit plasma by HPLC and its pharmacokinetics application. Asia-Pac. J. Pharmacol. 7, 53–56.

[6] Liang, J.W., Hsiu, S.L., Huang, H.C. and Lee-Chao, P.D. (1993) HPLC analysis of emodin in serum, herbs and Chinese herbal prescriptions. J. Food Drug Anal. 1, 251–257.

[7] Wasserman, L., Avigad, S., Beery, E., Nordenberg, J. and Fenig, E. (2002) The effect of aloe emodin on the proliferation of a new Merkel carcinoma cell line. Am. J. Dermatopathol. 24, 17–22.

[8] Fenig, E., Nordenberg, J., Beery, E., Sulkes, J. and Wasserman, L. (2004) Combined effect of aloe-emodin and chemotherapeutic agents on the proliferation of an adherent variant cell line of Merkel cell carcinoma. Oncol. Rep. 11, 213–217.

[9] Chen, H.C., Hsieh, W.T., Chang, W.C. and Chung, J.G. (2004) Aloe-emodin induced in vitro G2/M arrest of cell cycle in human promyelocytic leukemia HL-60 cells. Food Chem. Toxicol. 42, 1251–1257.

[10] Pecere, T., Gazzola, M., Mucignat, V., et al. (2000) Aloe-emodin is a new type of anticancer agent with selective activity against neuroectodermal tumors. Cancer Res. 60, 2800–2804.

[11] Saleem, R., Faizi, S., Siddiqui, B.S., et al. (2001) Hypotensive effect of chemical constituents from Aloe barbadensis. Planta Med. 67, 757–760.

[12] Yonemitsu, S., Nishimura, H., Shintani, M., et al. (2001) Troglitazone induces GLUT4 translocation in L6 myotubes. Diabetes 50, 1093–1101.

[13] Gayathri, B., Manjula, N., Vinay kumar, K.S., Lakshmi, B.S. and Balakrishnan, A. (2007) Pure compound from Boswellia serrata extract exhibits anti-inflammatory properties in human PBMC's and mouse macrophages through inhibition of TNF alpha, IL-1 beta, NO and MAP kinases. Int. Immunopharmacol. 7 (4), 473–482.

[14] Ambati, S., Kim, H.K., Yang, J.Y., Lin, J., Della-Fera, M.A. and Baile, C.A. (2007) Effects of leptin on apoptosis and adipogenesis in 3T3–L1 adipocytes. Biochem. Pharmacol. 73, 378–384.

[15] Merlijn, B., Peter, J.A. and Maassen, J.A. (2005) Genistein directly inhibits GLUT4 mediated glucose uptake in 3T3–L1 adipocytes. Biochem. Biophys. Res. Commun. 326, 511–514.

[16] Zhe, C., Pang, Tao., Min, Gu., et al. (2006) Berberine stimulated glucose uptake in L6 myotubes involves both AMPK and p38 MAPK. Biochim. Biophys. Acta 1760, 1682–1689.

[17] Muthusamy, V.S., Anand, S., Sangeetha, K.N., Sujatha, S., Arun, B. and Lakshmi, B.S. (2008) Tannins present in *Cichorium intybus* enhance glucose uptake and inhibit adipogenesis in 3T3–L1 adipocytes through PTP1B inhibition. Chem.-Biol. Interact. 174, 69–78.

[18] Tzeng, Y.-M., Chen, K., Rao, Y.K. and Lee, M.-J. (2009) Kaempferitrin activates the insulin signaling pathway and stimulates secretion of adiponectin in 3T3-L1 adipocytes. Mol. Cell. Pharmacol., doi:10.1016/j.ejphar.2009.01.023.

[19] Sangeetha, K.N., Sujatha, S., Muthusamy, V.S., Anand, S., Nithya, N., Velmurugan, D., Balakrishnan, Arun. and Lakshmi, B.S. (2010) 3β-taraxerol of Mangifera indica, a PI3K dependent dual activator of glucose transport and glycogen synthesis in 3T3–L1 adipocytes. Biochim. Biophys. Acta 1800, 359–366.

[20] Gould, G.W., Derechin, V., James, D.E., Tordjman, K., Ahern, S., Gibbs, E.M., Lienhard, G.E. and Mueckler, M. (1989) Insulin stimulated translocation of the HepG2/erythrocyte type glucose transporter expressed in 3T3 L1 adipocytes. J. Biol. Chem. 264, 2180–2184.

[21] Shepherd, P.R., Withers, D.J. and Siddle, K. (1998) Phosphoinositide 3 kinase. The key switch mechanism in insulin signaling. Biochem. J. 333, 471–490.

[22] Zierath, J.R., Krook, A. and Wallberg-Henriksson, H. (2000) Insulin action and insulin resistance in human skeletal muscle. Diabetologia 43 (7), 821–835.

[23] Whitehead, J.P., Clark, Sharon F., Urs, B. and James, David E. (2000) Signaling through the insulin receptor. Curr. Opin. Cell Biol. 12, 222–228.

[24] Laville, M., Auboeuf, D., Khalfallah, Y., Vega, N., Riou, J.P. and Vidal, H. (1996) Acute regulation by insulin of phosphotidylinositol-3-kinase, Rad, GLUT4 and lipoprotein lipase mRNA Levels in human muscle. J. Clin. Invest. 98, 43–49.

[25] Leng, Y., Karlsson, H.R. and Zierath, J.R. (2004) Insulin signaling defects in type 2 diabetes. Rev. Endocr. Metab. Disord. 5, 111–117.

[26] Ueki, K., Yamamoto-Honda, R., Kaburagi, Y., Yamauchi, T., et al. (1998) Potential role of protein kinase B in insulin-induced glucose transport, glycogen synthesis, and protein synthesis. J. Biol. Chem. 273 (9), 5315–5322.

[27] Cross, D.A., Alessi, D.R., Cohen, P., Andjelkovich, M. and Hemmings, B.A. (1995) Inhibition of glycogen synthase kinase- 3 by insulin mediated by protein kinase B. Nature 378, 785–789.

[28] Tanti, J.F., Grillo, S., Gremeaux, T., Coffer, P.J., Van Obberghen, E. and Le Marchand-Brustel, Y. (1997) Potential role of protein kinase B in glucose transporter 4 translocation in adipocytes. Endocrinology 138, 2005–2010.

[29] Ueki, K., Yamamoto-Honda, R., Kaburagi, Y., Yamauchi, T., Tobe, K., Burgering, B.M.T., Coffer, P.J., Komuro, I., Akanuma, Y., Yazaki, Y. and Kadowaki, T. (1998) Potential role of protein kinase B in insulin-induced glucose transport, glycogen synthesis, and protein synthesis. J. Biol. Chem. 273, 5315–5322.

[30] Gino, M.S., Pelaez, F. and Zhang, Bei B. (2001) Discovery of a small molecule insulin receptor activator. J. Endocrinol., 107–127.

[31] Jung, K.H., Choi, H.S., Kim, D.H., Han, M.Y., Chang, U.J., Yim, S.V., Song, B.C., Kim, C.H. and Kang, S.A. (2008) Epigallocatechin gallate stimulates glucose uptake through the phosphatidylinositol 3-kinase-mediated pathway in L6 rat skeletal muscle cells. J. Med. Food. 11 (3), 429–434.

[32] Sujatha, S., Anand, S., Sangeetha, K.N., Shilpa, K., Lakshmi, J., Balakrishnan, A. and Lakshmi, B.S. (2010) Biological evaluation of (3β)-STIGMAST-5-EN-3-OL as potent anti-diabetic agent in regulating glucose transport using in vitro model. Int. J. Diabetes Mellitus, doi:10.1016/j.ijdm.2009.12.013.

[33] Goodyear, L.J., Giorgino, F., Sherman, L.A., Carey, J., Smith, R.J. and Dohm, G.L. (1995) Insulin receptor phosphorylation, insulin receptor substrate-1 phosphorylation, and phosphatidylinositol 3-kinase activity are decreased in intact skeletal muscle strips from obese subjects. J. Clin. Invest. 95 (5), 2195–2204.

[34] Pessin, J., Thurmond, D., Elmendorf, J., Coker, K. and Andokada, S. (1999) 'Molecular basis of insulin-stimulated GLUT4 vesicle trafficking'. J. Biol. Chem. 274, 2593–2596.

[35] Klip, A. and Leiter, L.A. (1990) Cellular mechanism of action of metformin. Diabetes Care 13, 696–704.

[36] Jiang, Z.Y., Zhou, Q.L., Coleman, K.A., et al. (2003) Insulin signaling through Akt/protein kinase B analyzed by small interfering RNA-mediated gene silencing. Proc. Natl. Acad. Sci. USA 100, 7569–7574.
[37] Orena, S.J., Torchia, A.J. and Garofalo, R.S. (2000) Inhibition of glycogen synthase kinase 3 stimulates glycogen synthase and glucose transport by distinct mechanism in 3T3L1 adipocytes. J. Biol. Chem. 275, 15765–15772.
[38] Cross, D.A., Alessi, D.R., Cohen, P., Andjelkovich, M. and Hemmings, B.A. (1995) Inhibition of glycogen synthase 3 by insulin mediated by protein kinase B. Nature 378, 785–789.
[39] MacDougald, O.A. and Mandrup, S. (2002) Adipogenesis: forces that tip the scales. Trends Endocrinol. Metab. 13, 5–11.
[40] Sheng, X., Zhang, Y., Gong, Z., Huang, C. and Zang, Y.Q. (2008) improved insulin resistance and lipid metabolism by cinnamon extract through activation of peroxisome proliferator-activated receptors. PPAR Res., 581348.
[41] Pastromas, S. and Koulouris, S. (2006) Thiazolidinediones: antidiabetic drugs with cardiovascular effects. Hellenic J. Cardiol. 47, 352–360.
[42] Zhang, S. and Zhang, Z.-Y. (2007) PTP 1B as a drug target; recent developments in PTP 1B inhibitor discovery. Drug Discovery Today 12 (9–10).
[43] Bertrand, L., Ginion, A., Beauloye, C., Hebert, Alexandre D., Guigas, B., Hue, L. and Vanoverschelde, J.-L. (2006) AMPK activation restores the stimulation of glucose uptake in an in vitro model of insulin-resistant cardiomyocytes via the activation of protein kinase B. Am. J. Physiol. Heart Circ. Physiol. 291, H239–H250.
[44] Bjornholm, M., Kawano, Y., Lehtihet, M. and Zierath, J.R. (1997) Insulin receptor substrate-1 phosphorylation and phosphatidylonositol 3-kinase activity are decreased in skeletal muscle from NIDDM subjects following in vivo insulin stimulation. Diabetes 46, 524–527.
[45] Goodyear, W.T., Giorgino, F., Sherman, L.A., Carvey, J., Smith, R.J. and Dohm, G.L. (1995) Insulin receptor phosphorylation, insulin receptor substrate-1 phosphorylation and phosphatidylinositol 3- kinase activity are decreased in intact skeletal muscle strips from obese subjects. J. Clin. Invest. 95, 2195–2204.
[46] Rondinone, C.M., Trevillyan, J.M., Clampit, J., et al. (2002) Protein tyrosine phosphatase 1B reduction regulates adiposity and expression of genes involved in lipogenesis. Diabetes 51, 2405–2411.